

X-ray triple refraction and triple absorption in a cobalt-complex crystal

Kouhei Okitsu,^{a,*} Yoshinori Ueji,^b Takuyo Oguchi,^c Yuji Hasegawa,^{d,†} Yuji Ohashi^e and Yoshiyuki Amemiya^{d,‡}

^aNational Research Laboratory of Metrology, 1-1-4 Umezono, Tsukuba, Ibaraki 305, Japan, ^bDepartment of Synchrotron Radiation Science, The Graduate University for Advanced Studies, Tsukuba, Ibaraki 305, Japan, ^cRIKEN SPring-8, Kamigori, Ako-gun, Hyogo 678-12, Japan, ^dEngineering Research Institute, School of Engineering, The University of Tokyo, Yayoi, Bunkyo, Tokyo 113, Japan, and ^eDepartment of Chemistry, Tokyo Institute of Technology, Ookayama, Meguro, Tokyo 152, Japan. E-mail: yrt01404@niftyserve.or.jp

(Received 4 August 1997; accepted 13 January 1998)

X-ray triple refraction and triple absorption have been quantitatively measured for the first time. The samples were (100)-, (010)- and (001)-oriented plates of a cobalt-complex monoclinic crystal. The apparatus used was an energy-tunable X-ray polarimeter with a phase retarder. The X-ray energy was scanned over a range of 150 eV near the cobalt *K*-absorption edge. Both the spectra of ellipticity and rotation of polarization were completely different for each crystal plate, which revealed that the biaxial crystal had three refractive indices and three absorption coefficients in the X-ray region. The Kramers–Kronig relation between the real and imaginary parts of the dielectric anisotropy has been quantitatively confirmed for all three different orientations.

Keywords: X-ray polarimeters; polarization interferometry; polarized XAFS; X-ray triple refraction; X-ray trichroism.

1. Introduction

Since the work of Templeton & Templeton (1980, 1982, 1985) on X-ray anisotropic absorption, it has been recognized that anisotropic crystals have two absorption coefficients depending on the polarization state of incident X-rays near absorption edges. However, biaxial features of anisotropic crystals, which might have three absorption coefficients and three refractive indices, have not yet been clarified.

Recently, Okitsu *et al.* (1996) have successfully measured X-ray linear birefringence and linear dichroism in a hexagonal cobalt crystal using a new type of energy-tunable X-ray polarimeter (Okitsu *et al.*, 1996, 1998). This X-ray polarimeter design was based on an X-ray energy-tunable polarimeter (Siddons *et al.*, 1990; Hart *et al.*, 1991) consisting of a Hart–Rodrigues polarizer and analyser (Hart & Rodrigues, 1979). A remarkable feature of this new type of X-ray polarimeter is that a transmission-type X-ray phase retarder (Hirano *et al.*, 1993, 1994, 1995) is introduced as a third optical device, in addition to the Hart–Rodrigues polarizer and analyser. Not only the magnitude but also the sign of

* Present address: Engineering Research Institute, School of Engineering, The University of Tokyo, Yayoi, Bunkyo, Tokyo 113, Japan.

† Present address: Department of Applied Physics, School of Engineering, The University of Tokyo, Hongo, Bunkyo, Tokyo 113, Japan.

the refraction anisotropy of a cobalt crystal in the X-ray region was successfully obtained, owing to the well defined elliptically polarized incident X-rays produced by the phase retarder (Okitsu *et al.*, 1996, 1998).

In this paper, X-ray triple refraction and triple absorption, measured for the first time using the new X-ray energy-tunable polarimeter, will be described.

2. Experimental

Fig. 1 shows a schematic drawing of the new type of X-ray energy-tunable polarimeter. Details of the optical system have been described in other papers (Okitsu *et al.*, 1996, 1998). (100)-, (010)- and (001)-oriented plates of a cobalt-complex crystal, [(*S*)-1-cyanoethyl][(*S*)-phenylethylamine]cobaloxime, which belongs to the monoclinic crystal system, were prepared as samples. The lattice parameters are as follows: $a = 8.777 \text{ \AA}$, $b = 13.390 \text{ \AA}$, $c = 9.540 \text{ \AA}$, $\beta = 96.79^\circ$ (Takenaka *et al.*, 1993).

The (100) plate, which was about 300 μm thick, was set so that the a axis of the crystal was parallel to the beam direction and the c axis was inclined by 20° from the direction of the major axis of the incident elliptical polarization from the phase retarder. The (010)-plate, which was about 500 μm thick, was set so that the b axis of the crystal was parallel to the beam direction and the a axis was inclined by 23° from the direction of the major axis of polarization. The (001)-plate, which was about 300 μm thick, was set so that the c axis was parallel to the beam direction and the b axis was inclined by 45° from the direction of the major axis. The ellipticity of polarization of the incident X-rays was controlled to be ± 0.03 for the a - and c - plates and ± 0.035 for the b -plate during the energy scan by changing the reflection angle of the phase retarder based on calculations from dynamical diffraction theory. The intensity of the outgoing X-ray beam from the analyser was measured at 17 analyser angular positions with a step of 900 arcsec in a range of $\pm 2^\circ$ around the beam direction from the crossed-nicol position. The X-ray intensity at each angular position of the analyser was measured for 20 s. The ellipticity and rotation of polarization were determined by a least-square fit (see Okitsu *et al.*, 1998) which describes X-ray linear birefringence and linear dichroism. The X-ray energy was scanned over a range of about 150 eV in the vicinity of the cobalt *K*-absorption edge, with a step of about 1 eV.

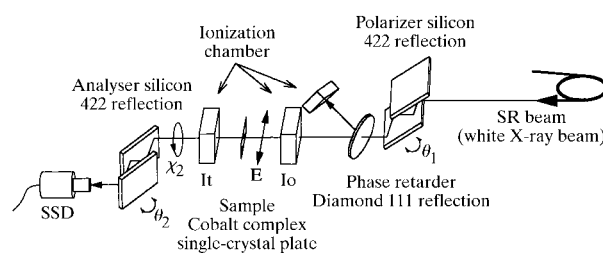


Figure 1

Experimental arrangement of the new type of X-ray energy-tunable polarimeter with a phase retarder. The polarizer and analyser crystals are similar channel-cut crystals giving four-bounce 422 symmetric Bragg reflections and are equipped with a Hart–Rodrigues offset mechanism. The phase retarder is a diamond (001)-oriented plate of 313 μm thickness giving 111 asymmetric Laue-case reflection with a plane of incidence inclined by 45° from the horizontal. The X-ray energy was scanned by controlling the polarizer, analyser and phase-retarder crystals simultaneously.

3. Results and discussion

Figs. 2(a), 2(b) and 2(c) show ellipticity spectra for the (100) plate, the (010) plate and for the (001) plate samples, respectively. These spectra are clearly different from one another, indicating that the monoclinic crystal has three refractive indices; *i.e.* triple refraction is taking place in the crystal. Reversed polarization ellipticity spectra have also been obtained using an incident X-ray beam with reversed helicity, but are not shown in this paper. Triple refraction in the X-ray frequency region has been detected and measured quantitatively for the first time.

Figs. 3(a), 3(b) and 3(c) show polarization-rotation spectra for the (100)-, (010)- and (001)-oriented plates, respectively, caused by the difference in absorption coefficients in the *a*-, *b*- and *c*-axis directions of the crystal. Identical spectra corresponding to (a), (b) and (c) were obtained when the polarization helicity of the incident X-ray beam was reversed. Triple absorption (trichroism) in the X-ray frequency region has been detected and measured quantitatively for the first time.

Fig. 4 shows spectra of the imaginary part of the dielectric constant anisotropy between (a) the *b*- and *c*-axis directions, (b) the *c*- and *a*-axis directions and (c) the *a*- and *b*-axis directions, calculated from the ellipticity and the rotation of polarization, together with the Kramers–Kronig transforms of the real part of the dielectric constant anisotropy. The right and left ordinates in Figs. 4(a), 4(b) and 4(c) are shifted for clarity and are drawn on an

absolute scale of relative dielectric constant (no procedure for scaling was made).

The procedure for calculating the real and imaginary parts of the dielectric anisotropy is as follows. First, consider an elliptical polarization with an ellipticity R_0 , the major axis of which is inclined by θ from the optical *x* axis in an *xy* orthogonal coordinate system in the sample crystal. $D_x^{(0)}$ and $D_y^{(0)}$, the amplitudes of the incident X-rays in the *x* and *y* directions, are given by

$$\begin{pmatrix} D_x^{(0)} \\ D_y^{(0)} \end{pmatrix} = \begin{pmatrix} \cos \theta & -\sin \theta \\ \sin \theta & \cos \theta \end{pmatrix} \begin{pmatrix} 1 \\ -R_0 i \end{pmatrix} \quad (1)$$

$$= \begin{pmatrix} \cos \theta + R_0 i \sin \theta \\ \sin \theta - R_0 i \cos \theta \end{pmatrix}. \quad (2)$$

X-rays transmitted through the sample crystal can be represented in a similar way by

$$\begin{pmatrix} D_x \\ D_y \end{pmatrix} = \begin{pmatrix} D_x^{(0)} \exp[-2\pi i(n_x - 1)z/\lambda] \\ D_y^{(0)} \exp[-2\pi i(n_y - 1)z/\lambda] \end{pmatrix} \quad (3)$$

$$= \begin{pmatrix} \cos(\theta + \alpha) + Ri \sin(\theta + \alpha) \\ \sin(\theta + \alpha) - Ri \cos(\theta + \alpha) \end{pmatrix}. \quad (4)$$

Here, D_x and D_y are the amplitudes of X-rays transmitted through the sample crystal in the *x* and *y* directions, λ is the X-ray wavelength, n_x and n_y are the complex refractive indices for polarization in the *x* and *y* directions, z is the sample thickness and R and α

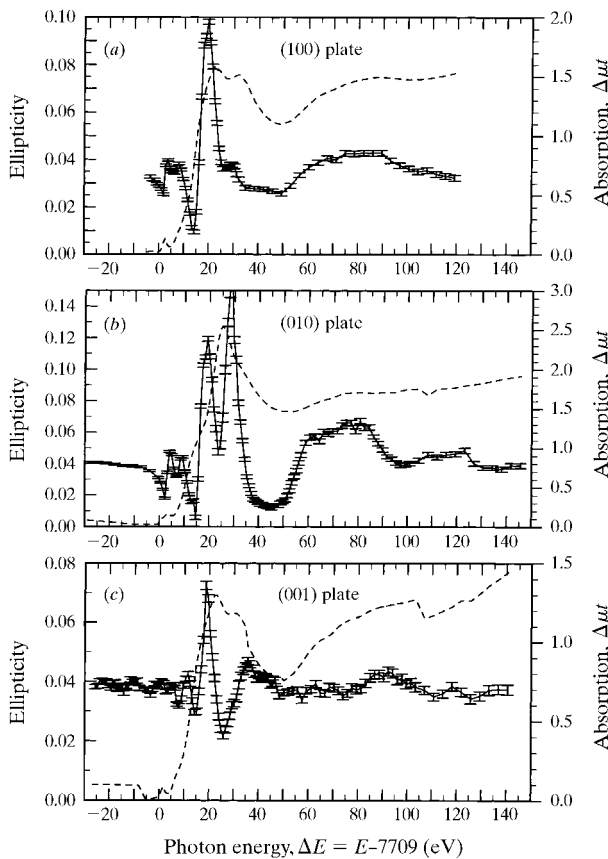


Figure 2

Spectra of ellipticity of polarization of an X-ray beam transmitted through (a) (100)-, (b) (010)- and (c) (001)-oriented plate crystals. The ellipticity of polarization of the incident X-ray beam produced by the phase retarder was set to be (a) +0.03, (b) +0.035 and (c) +0.03. The clear difference between the spectra in (a), (b) and (c) reveals that X-ray triple refraction is taking place in the monoclinic crystal.

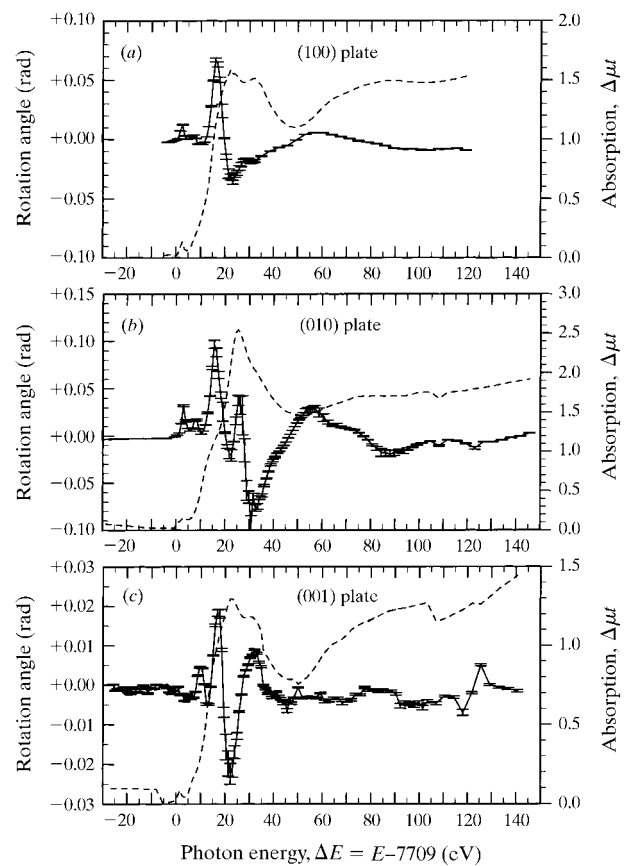


Figure 3

Spectra of rotation of polarization of an X-ray beam transmitted through (a) (100)-, (b) (010)- and (c) (001)-oriented plate crystals. The ellipticity of the incident X-ray beam produced with the phase retarder was (a) +0.03, (b) +0.035 and (c) +0.03. The clear difference between the spectra in (a), (b) and (c) reveals that X-ray triple absorption (trichroism) is taking place in the monoclinic crystal.

are the ellipticity and rotation of polarization, respectively. Dividing D_x by D_y gives

$$D_x/D_y = (D_x^{(0)}/D_y^{(0)}) \exp(-2\pi i \Delta n z/\lambda) \quad (5)$$

$$= \frac{\cos(\theta + \alpha) + Ri \sin(\theta + \alpha)}{\sin(\theta + \alpha) - Ri \cos(\theta + \alpha)}, \quad (6)$$

where $\Delta n = n_x - n_y$. Similarly, dividing $D_x^{(0)}$ by $D_y^{(0)}$ gives

$$D_x^{(0)}/D_y^{(0)} = (\cos \theta + R_0 i \sin \theta)/(\sin \theta - R_0 i \cos \theta). \quad (7)$$

Comparing (5), (6) and (7), we obtain the following relations:

$$\exp(-2\pi i \Delta n z/\lambda) = B, \quad (8)$$

$$B \equiv \frac{[\cos(\theta + \alpha) + Ri \sin(\theta + \alpha)](\sin \theta - R_0 i \cos \theta)}{[\sin(\theta + \alpha) - Ri \cos(\theta + \alpha)](\cos \theta + R_0 i \sin \theta)}. \quad (9)$$

If the real and imaginary parts of Δn are denoted by $\Delta n^{(r)}$ and $\Delta n^{(i)}$ then

$$\exp(-2\pi i \Delta n z/\lambda) = \exp(-2\pi i \Delta n^{(r)} z/\lambda) \exp(2\pi \Delta n^{(i)} z/\lambda). \quad (10)$$

Comparing (8), (9) and (10), we obtain

$$-2\pi \Delta n^{(r)} z/\lambda = \arg B, \quad (11)$$

$$\exp(2\pi \Delta n^{(i)} z/\lambda) = |B|. \quad (12)$$

Here, $\arg B$ and $|B|$ are the argument and the absolute value of the complex value B , as defined by (9). The real and imaginary parts of the relative dielectric constant anisotropy, $\Delta \varepsilon^{(r)}$ and $\Delta \varepsilon^{(i)}$, are given by

$$\Delta \varepsilon^{(r)} = 2\Delta n^{(r)}, \quad (13)$$

$$\Delta \varepsilon^{(i)} = 2\Delta n^{(i)}. \quad (14)$$

Spectra shown in Figs. 4(a), 4(b) and 4(c) were calculated by using (9) and (11)–(14). The Kramers–Kronig transforms were obtained by numerical integration.

We cannot give any explanation of the physical origin of the spectra in Figs. 2, 3 and 4 at present. However, data analysis to extract physical information related to the crystal structure is now in progress.

4. Conclusions

X-ray triple refraction and triple absorption (trichroism) have been detected and measured quantitatively for the first time using a new type of X-ray energy-tunable polarimeter with a phase retarder. The Kramers–Kronig relation was confirmed quantitatively between the real and imaginary parts of the dielectric anisotropies.

The authors wish to thank Professor M. Hart of Brookhaven National Laboratory for providing them with the polarizer and analyser crystals. They are also indebted to Dr K. Hirano of the Photon Factory for providing a diamond crystal for the phase retarder and a computer program giving the phase retardation. The present work was performed under the approval of the Photon Factory Program Advisory Committee (Proposal No.

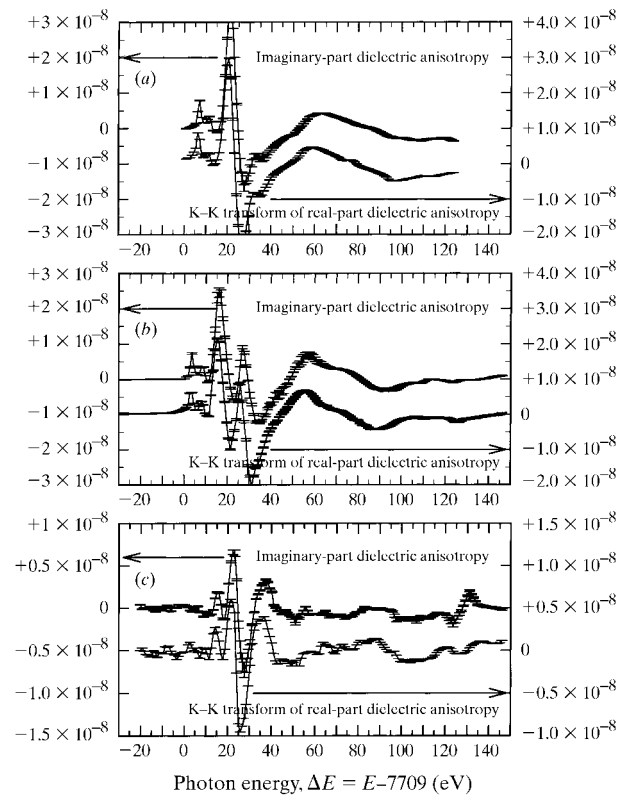


Figure 4

Spectra of the imaginary part of the dielectric anisotropy between (a) the *b*- and *c*-axis directions, (b) the *c*- and *a*-axis directions and (c) the *a*- and *b*-axis directions of the monoclinic sample crystal, calculated from the spectra of ellipticity and rotation of polarization, and the Kramers–Kronig (K–K) transforms of the imaginary part of the dielectric anisotropy. The left and right ordinates of each graph are shifted for clarity and are drawn on the absolute scale of relative dielectric constant.

95G-298) and was supported by a Grant-in-Aid for COE Research.

References

- Hart, M. & Rodrigues, A. R. D. (1979). *Philos. Mag. B*, **40**, 149–157.
- Hart, M., Siddons, D. P., Amemiya, Y. & Stojanoff, V. (1991). *Rev. Sci. Instrum.* **62**, 2540–2544.
- Hirano, K., Ishikawa, T. & Kikuta, S. (1993). *Nucl. Instrum. Methods Phys. Res. A*, **336**, 343–353.
- Hirano, K., Ishikawa, T. & Kikuta, S. (1995). *Rev. Sci. Instrum.* **66**, 1604–1609.
- Hirano, K., Ishikawa, T., Nakamura, I., Mizutani, M. & Kikuta, S. (1994). *Jpn. J. Appl. Phys.* **33**, L689–L692.
- Okitsu, K., Oguchi, T., Maruyama, H. & Amemiya, Y. (1996). *Proc. SPIE*, **2873**, 100–104.
- Okitsu, K., Oguchi, T., Maruyama, H. & Amemiya, Y. (1998). *J. Synchrotron. Rad.*, **5**, 995–997.
- Siddons, D. P., Hart, M., Amemiya, Y. & Hastings, J. B. (1990). *Phys. Rev. Lett.* **64**, 1967–1970.
- Takenaka, Y., Kojima, Y. & Ohashi, Y. (1993). *Acta Cryst.* **B49**, 852–859.
- Templeton, D. H. & Templeton, L. K. (1980). *Acta Cryst.* **A36**, 237–241.
- Templeton, D. H. & Templeton, L. K. (1982). *Acta Cryst.* **A38**, 62–67.
- Templeton, D. H. & Templeton, L. K. (1985). *Acta Cryst.* **A41**, 133–142.